



**ARTICLE**

# A New DOPO-Eugenol Adduct as an Effective Flame Retardant for Epoxy Thermosets with Improved Mechanical Properties

Daqin Zhang<sup>1,2</sup>, Chufeng Yang<sup>3</sup>, Huayang Ran<sup>1,2</sup>, Juanli Wang<sup>1,2,\*</sup>, Jintao Wan<sup>1,2,\*</sup>, Yuhu Li<sup>1,2</sup>, Pujun Jin<sup>1,2</sup> and Daodao Hu<sup>1,2</sup>

<sup>1</sup>School of Materials Science and Engineering, Shaanxi Normal University, Xi'an, 710119, China

<sup>2</sup>Engineering Research Center of Historical and Cultural Heritage Protection, Ministry of Education, Shaanxi Normal University, Xi'an, 710119, China

<sup>3</sup>Hangzhou First Applied Material Co., Ltd., Hangzhou, 311300, China

\*Corresponding Authors: Juanli Wang. Email: wangjuanli@snnu.edu.cn; Jintao Wan. Email: wanjintao@snnu.edu.cn

Received: 15 August 2021 Accepted: 08 October 2021

## ABSTRACT

The development of efficient green flame retardants is an important way to realize more sustainable epoxy thermosets and downstream materials. In this work, a monoepoxide is synthesized through O-glycidylation of eugenol, and then reacted with DOPO (9,10-dihydro-9-oxa-10-phosphophenanthrene-10-oxide) to obtain a new bio-based flame retardant, DOPO-GE. DOPO-GE is blended with a bisphenol A epoxy prepolymer exhibiting good compatibility and DDS (4,4'-diaminodiphenylsulfone) is used as the curing agent to afford epoxy thermosets. Although DOPO-GE leads to the reduced glass transition temperature of the thermosets, the storage modulus increases considerably. The DOPO-GE-modified thermosets exhibit the high thermal stability with the onset thermal decomposition temperature in nitrogen and air exceeding 300°C. When the phosphorus content in the thermoset is 1.0%, the residual yield of the thermosets at 750°C in nitrogen increases from 13.9% to 30.6%, due to the increased charring ability. More interestingly, when the phosphorus content is only 0.5%, the limiting oxygen index is as high as 30.3% with UL94 V0 achieved. Cone calorimeter results reveals the significantly decreased heat release rate, total heat release, mass loss and total smoke production. Furthermore, DOPO-GE can notably improve the flexural strength, flexural modulus and fracture toughness, whereas the shear and impact strength are reduced to varied extents. In short, DOPO-GE can be obtained via a facile way, and shows the good flame-retardant effect on the epoxy thermosets with an application potential.

## KEYWORDS

Flame retardant; epoxy thermosets; bio-based additives; performances

## 1 Introduction

Epoxy resins are widely used in many fields mainly because of their excellent mechanical properties, insulation properties and good processability. Bisphenol A-based epoxy resin (DGEBA) is the most commonly used epoxy prepolymer, accounting for more than 80% market share of the whole epoxy resin market. However, DGEBA is flammable and easy to burn in air. Therefore, improving the flame retardancy of DGEBA is a very important issue for a number of applications, and thus becomes a hot



research topic in academia and industry. Many methods have been used to improve the flame retardancy of DGEBA. For example, brominated epoxy resins have high intrinsic flame retardancy, but they produce highly toxic gases in combustion. Therefore, halogen-free flame retardants for epoxy is of particular importance. For example, aluminum hydroxide, magnesium hydroxide and other inorganic fillers are added to the epoxy systems to improve flame retardancy, but such inorganic flame retardants usually need a high loading, resulting in problems regarding processing and compatibility. Therefore, developing organic flame retardants with better compatibility and higher efficiency provides an alternative solution to the above problems. In particular, organic flame retardants based on DOPO (9,10-dihydro-9-oxa-10-phosphophenanthrene-10-oxide) have the advantages of high flame retardancy, low volatilization, low moisture absorption, good transparency, good compatibility, and reasonable costs, so that DOPO functions as the very useful building block to develop many new and efficient flame retardants for polymeric materials including epoxy thermosets [1–8].

In order to reduce the impact on environment and relieve resource shortage, the development of renewable epoxy resin and related flame retardants has attracted more and more attention. In recent years, many studies on the synthesis of epoxy thermosets and related flame retardants by replacing bisphenol A with bio-based phenols have been reported extensively, such as cardanol [9–13], vanillin [14–16], magnolol [17,18], ellagic acid [19], syringaldehyde [20], and eugenol, to name a few. Among them, eugenol is of particular interest. Eugenol is a natural substituted phenolic compound. Its molecules contain such active groups as allyl and phenolic hydroxyl groups. Eugenol can be chemically functionalized to obtain a variety of bio-based thermoplastics and thermosets, additives, and functional polymeric materials [21–62]. At the same time, a number of publications address eugenol-based flame-retardant epoxy systems. For example, the phenolic group of eugenol is used to react with different linkers such as phosphorus containing organic compounds to produce di-, tri- or multi-allyl compounds, and then the corresponding di-, tri- or multi-functional epoxy monomers or oligomers are obtained by epoxidation of the allyl groups [63–66]. Certainly, DOPO is an efficient epoxy flame retardant, but to our knowledge, DOPO-modified eugenol is still not applied as the flame retardant for epoxy thermosets.

In this paper, eugenol is undergone O-glycidylation to introduce a highly reactive terminal epoxy group, and then reacted with phosphorus hydrogen bond of DOPO to obtain a DOPO-modified eugenol-based flame retardant (DOPO-GE). DOPO-GE is used to modify commercially available DGEBA, and 4,4'-diaminodiphenylsulfone (DDS) is used as the curing agent to obtain the thermosets. We systematically study the dynamic mechanical properties, thermal decomposition behavior, flame retardancy, mechanical properties and fracture behavior of the thermosets. It is found that DOPO-GE is very effective to improve the flame retardancy and can increase the rigidity of the obtained epoxy materials simultaneously.

## 2 Experimental

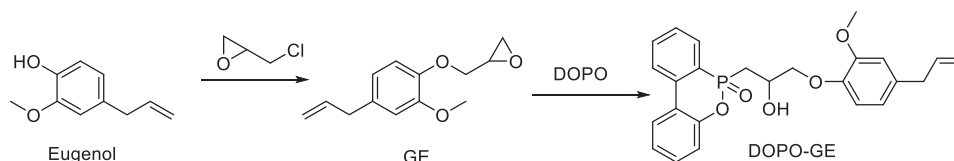
### 2.1 Reagents and Raw Materials

Eugenol was purchased from a commercial source, and decolorized by vacuum distillation before use. Fresh-distilled eugenol is a colorless liquid with a purity of +99% (GC). Epichlorohydrin, sodium hydroxide, benzyltriethylammonium chloride and methanol were purchased from Sinopharm. 4,4'-Diaminediphenylsulfone (99%) was obtained from Energy Chemical. Commodity bisphenol A epoxy resin (E54<sup>TM</sup>) with epoxy value of 0.556 mol/100 g was used in this study. Unless there were other special specifications, all the chemicals and materials were used as received.

### 2.2 Synthesis of Flame Retardants

As shown in [Scheme 1](#), add eugenol (100 g, 0.61 mol), 2.53 g of benzyltriethylammonium chloride and epichlorohydrin (500 ml) into a 1000 ml flask in a water bath. After reacting at 80°C for 6 hours, the flask was rotary evaporated to remove unreacted epichlorohydrin up to <10 mbar for 30 min. The remainder was dissolved into 500 ml of toluene, and then 40% sodium hydroxide solution (24.4 g of NaOH) was added

dropwise at room temperature with stirring for 6 h. The upper organic layer was separated, extracted with deionized water several times until neutrality, and dried over anhydrous sodium sulfate overnight. After removal of the solvent in a vacuum oven at 80°C overnight, the obtained crude product was dissolved in methanol and chilled to yield white crystals. The collected crystals were dried in a vacuum to obtain glycidyl ether of eugenol (GE) in a ~70% yield.



**Scheme 1:** Synthesis of glycidyl ether of eugenol and its DOPO adduct

DOPO (62.30 g, 0.28 mol) and glycidyl ether of eugenol (62.40 g, 0.28 mol) were charged into a 500 ml flask and heated in an oil bath (170°C) with stirring to obtain a clear solution. Then triphenylphosphine (0.31 g) was added and reacted for 28 h to obtain a viscous liquid without further separation as the bio-based flame retardant (DOPO-GE) in a quantitative yield.

### 2.3 Preparation of Cured Thermosets

To a preheated (135°C) mold sprayed with releasing agent, a quantitative mixture sample of E54, DDS, and DOPO-GE were filled and degassed under reduced pressure. The following curing procedures were carried out: 180°C for 2 h, 200°C for 4 h, and 220°C for 4 h, and then cooled to room temperature. Disassemble the mold and machine the cured thermosets into desired dimensions for further testing. The typical formulations of the epoxy thermosets are listed in [Table 1](#).

**Table 1:** Typical formulations of epoxy thermosets in this study

	E54/g	DDS/g	DOPO-GE/g	P/wt%
E54/DDS	35.0	12.0	0	0
E54/DDS/0.5%P	35.0	12.0	3.49	0.5
E54/DDS/1.0%P	35.0	11.9	7.71	1.0
E54/DDS/1.5%P	35.0	12.0	12.6	1.5
E54/DDS/2.0%P	35.0	12.0	18.4	2.0

### 2.4 Characterizations

**Infrared spectroscopy (FT-IR).** A spectrophotometer (PerkinElmer Spectrum Two UATR) was used to register IR spectra. Potassium bromide was used as the supporter and wavenumber range was 4000–500  $\text{cm}^{-1}$ .

**Nuclear magnetic resonance (NMR).** A nuclear magnetic resonance spectrometer (400 MHz, JEOL) was used to acquire the  $^1\text{H}$  NMR spectra of the samples with deuterated chloroform ( $\text{CDCl}_3$ ) as the solvent and tetramethylsilane as the internal standard, and the number of scans was 8 times.

**Thermogravimetric analysis.** A thermal analysis system instrument (Q600, TA Instruments) was used to analyze the thermal decomposition of the cured epoxy samples. An appropriate amount (4–5 mg) of the cured epoxy thermoset was heated from room temperature at a heating rate of 20 K/min to 800°C in an air and a nitrogen atmospheres, respectively.

**Dynamic mechanical thermal analysis (DMA).** A DMA analyzer (Q800, TA instruments) was used to analyze the viscoelasticity of the cured epoxy thermosets. The sample (60 mm × 10 mm × 2.6 mm) was fixed

on the dual-cantilever beam, the amplitude was 25  $\mu\text{m}$ , the frequency was 1 Hz, and the heating rate was 3 K/min from room temperature to 300°C.

**Shear strength.** A universal testing machine (RGM-2010, Regal Instrument, Ltd., China) was used to measure the shear strength according to ISO 527-2012 with the tensile speed of 10 mm/min. The epoxy adhesive was coated on a steel plate with bonding surface of 12.5 mm  $\times$  25 mm, and cured at 180°C for 6 h.

**Flexural properties.** Testing of flexural properties of the cured epoxy was conducted on the universal testing machine. According to the national standard GB/T 9341-2008, the polished specimens were measured at room temperature with the crosshead speed of 5 mm/min.

**Impact strength.** An impact tester (XJJD-5, Chengde Jinjian Testing Instrument, China) was used to determine impact strength of V-notched specimens according to GB/T 2571-1995. The impact speed was 2.9 m/s and the impact energy (2 J).

**Fracture toughness and fracture energy.** The universal testing machine was used to measure the fracture toughness and fracture energy according to ASTM D5045. The processed samples (length 60  $\pm$  0.02 mm, width 10  $\pm$  0.02 mm, thickness 5  $\pm$  0.02 mm, and notch 4  $\pm$  0.02 mm) were tested at the crosshead speed of 10 mm/min in bending mode.

**Limiting oxygen index (LOI).** An oxygen index tester (JF-5, Fujian Survey Instrument and Equipment, China) was used to determine the LOI values in terms of ISO 4589-1996. UL 94 vertical burning test was carried out on the cured epoxy samples. A cone calorimeter (Fire Testing Technology) test was used to study flame retardancy the samples (100 mm  $\times$  100 mm  $\times$  4 mm) at a fixed heat flux of 35 kW/m<sup>2</sup> according to ISO 5660.

**Scanning electron microscope (SEM).** A SEM equipment (SU3500, Hitachi, Japan) was used to check the surface morphology of the residue of the samples after burning in the air. Gold was sprayed on the surface of the samples and the accelerating voltage applied was 5 KV.

### 3 Results and Discussion

#### 3.1 Molecular Characterization

As shown in Fig. 1A, DOPO has the infrared absorption at  $\sim$ 2400  $\text{cm}^{-1}$  due to the stretching vibration of phosphorus hydrogen (P-H) bonds, whereas DOPO-GE shows no absorption associated with P-H bond. Meanwhile, for DOPO-GE there is a strong hydroxyl stretching vibration between 3500–3000  $\text{cm}^{-1}$ , which is due to the ring-opening reaction between the epoxy group and the P-H bond [67]. Moreover, DOPO-GE displays a strong stretching vibration owing to the carbon-carbon double bond at  $\sim$ 1632  $\text{cm}^{-1}$ , indicating that the allyl double bond of GE has not changed. In addition, from <sup>1</sup>H NMR spectra (Fig. 2B) the signals of the allyl double on the product are observed at about 4.9 and 5.8 ppm, and the resonance of P-H bond at about 8.9 ppm in DOPO disappears, which further confirms that the P-H bond of DOPO has reacted with epoxy group of GE via a ring-opening process.

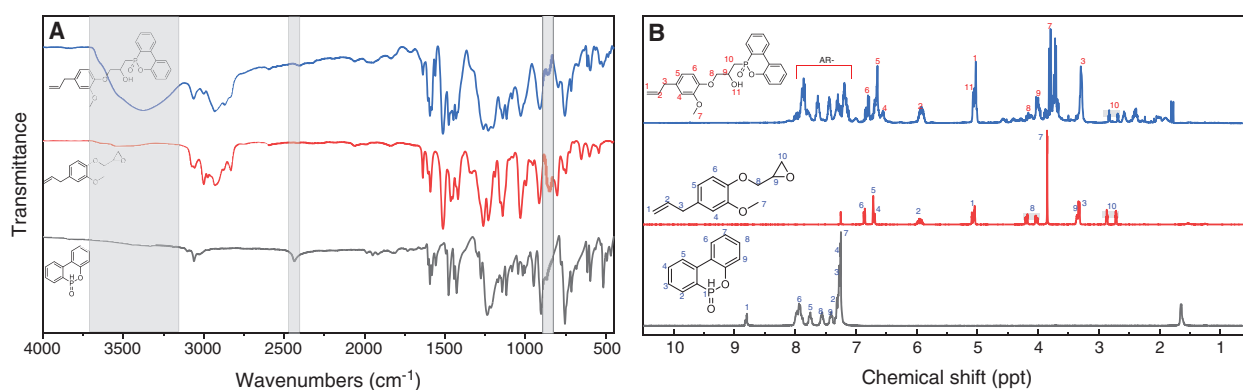


**Figure 1:** FTIR (A) and <sup>1</sup>H-NMR (B) spectra of DOPO, GE and DOPO-GE in CDCl<sub>3</sub>

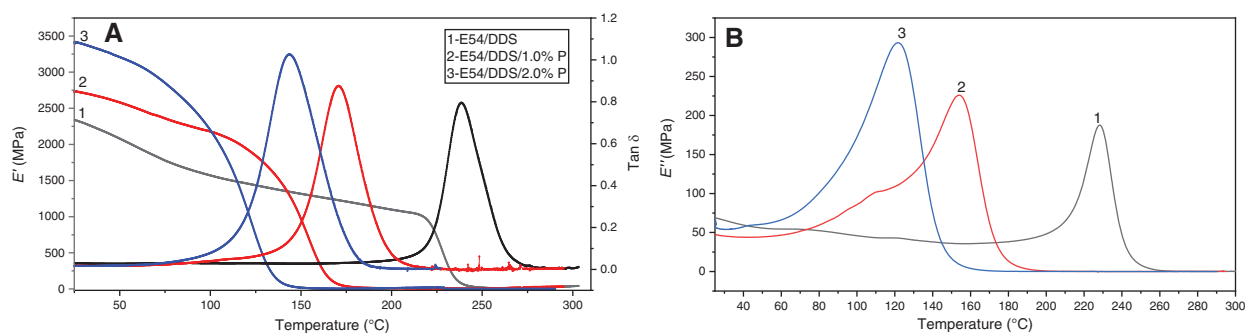


**Figure 2:** Dynamic mechanical properties (storage modulus  $E'$ , loss modulus  $E''$  and loss factor  $\text{Tan } \delta$ ) as function of temperature for E54/DDS, E54/DDS/1.0%P and E54/DDS/2.0%P thermosets

### 3.2 Dynamic Mechanical Properties of Thermosets

Fig. 2 shows the relationship between the dynamic mechanical properties (storage modulus  $E'$  and loss factor  $\text{Tan } \delta$ ) and temperature of the thermosets, E54/DDS, E54/DDS/1.0%P and E54/DDS/2.0%P. In a certain temperature range (below  $\sim 110^\circ\text{C}$ ),  $E'$  of E54/DDS/1.0%P and E54/DDS/2.0%P is higher than that of pristine E54/DDS, and increases with the DOPO-GE contents. For example, at  $25^\circ\text{C}$ ,  $E'$  of E54/DDS/2.0%P is the highest up to 3421 MPa, while the  $E'$  of DGEBA/DDS is the lowest (2339 MPa). At  $100^\circ\text{C}$ ,  $E'$  of E54/DDS/1.0%P and E54/DDS/2.0%P systems exceeds 2.1 GPa, while the  $E'$  of E54/DDS system does not exceed 1.6 GPa. Therefore, the addition of DOPO-GE can increase the rigidity of the cured thermosets within a relatively lower temperature range. The reason lies in that DOPO-GE provides condensed rigid aromatic segments with a stronger intermolecular interaction, and the allyl groups could react into the thermosetting network, which makes the motion of the molecular segments more difficult.

Fig. 2 shows that with the further increase of temperature,  $E'$  of thermoset decreases greatly in a certain temperature range, and the dissipation factor ( $\text{Tan } \delta$ ) and loss modulus ( $E''$ ) increase dramatically reaching their maximum, and then decreases rapidly approaching zero. This observation mean that the materials undergo the glass transition. The temperature for  $\text{Tan } \delta_{\text{max}}$  is taken as the glass transition temperature ( $T_g$ ). It can be found that with the increase of DOPO-GE fraction,  $\text{Tan } \delta_{\text{max}}$  of decreases gradually, while the glass-transition temperature range widens. Correspondingly, as shown in Table 2,  $T_g$  decreases from  $238.6^\circ\text{C}$  for E54/DDS to  $143.8^\circ\text{C}$  for the thermoset with 2.0%P content, indicating that DOPO-GE has strong plasticizing effect to tailor the glass transition temperature of the resultant thermosets. Interestingly, E54/DDS/1.0%P and E54/DDS/2.0%P show a higher rubbery modulus, likely due to allyl's polymerization which produces additional crosslinks [18].

**Table 2:** Storage modulus ( $E'$ ), loss modulus ( $E''$ ) and dissipation factor ( $\text{Tan } \delta$ ) of E54/DDS, E54/DDS/1.0%P and E54/DDS/2.0%P thermosets

Formulation	E54/DDS	E54/DDS/1.0%P	E54/DDS/2.0%P
$T_g, \text{Tan } \delta_{\text{(max)}}/^\circ\text{C}$	238.6	170.9	143.8
$\text{Tan } \delta_{\text{max}}$	0.797	0.876	1.026
$E''_{\text{max}}/\text{MPa}$	187.7	226.0	293.3
$E'_{25}/\text{MPa}$	2339	2719	3421
$E''_{25}/\text{MPa}$	68.93	47.77	56.55

(Continued)

Formulation	E54/DDS	E54/DDS/1.0%P	E54/DDS/2.0%P
$E'_{100}$ /MPa	1571	2179	2199
$E''_{100}$ /MPa	45.95	85.83	172.3
$E'_{\text{rubber}}$ /MPa	0.322	0.615	0.599

Note:  $E'_{\text{rubber}}$  is referred to the storage modulus at  $T_g + 30^\circ\text{C}$ .

### 3.3 Thermal Decomposition Behaviors

The effect of DOPO-GE on the thermal decomposition behavior of the cured epoxy resin in nitrogen and air is studied, see Fig. 3. The characteristic thermal decomposition temperatures, such as the onset, 5%, the thermal decomposition temperatures corresponding to the maximum decomposition rate ( $T_{\text{onset}}$ ,  $T_{d5}$  and  $T_{d\text{max}}$ ), and the residual fraction at  $750^\circ\text{C}$  are listed in Table 3. With the increased fraction of DOPO-GE,  $T_{\text{onset}}$  decreases likely due partially to the dissociation of the methyl functions inherited from DOPO-GE [67]. Nevertheless, all the systems have high thermal stability, no apparent thermal degradation occurs below  $250^\circ\text{C}$ , and  $T_{d5}$  and  $T_{\text{onset}}$  exceed  $300^\circ\text{C}$ . These results show that the thermal stability of the material can fully meet the requirements as a hard plastic, because the decomposition temperature is much higher than  $T_g$ . Specifically, in air, with the increase of DOPO-GE loading, the thermal decomposition temperatures decrease gradually, whereas the residual fraction shows a trend of first increasing and then decreasing. Accordingly, when the phosphorus content is 1.0%, the thermoset reaches its maximum residual yield, so DOPO-GE has an optimal content. The DOPO units from DOPO-GE can catalyze the dehydration of the epoxy. At the same time, organic phosphorus will transform into phosphoric acids after pyrolyzation, which can significantly catalyze the carbonization of the polymer matrix [68]. In air, the respective characteristic thermal decomposition temperatures of the systems, in general, decrease as compared with the case of  $\text{N}_2$ , and the effect of phosphorus content is also similar to that of the system in  $\text{N}_2$  during the first-step of decomposition. However, the thermal decomposition in the air shows two distinct steps. After the first step, the epoxy is carbonized, and the carbon formed in the second step will burn in the air and produce soot.

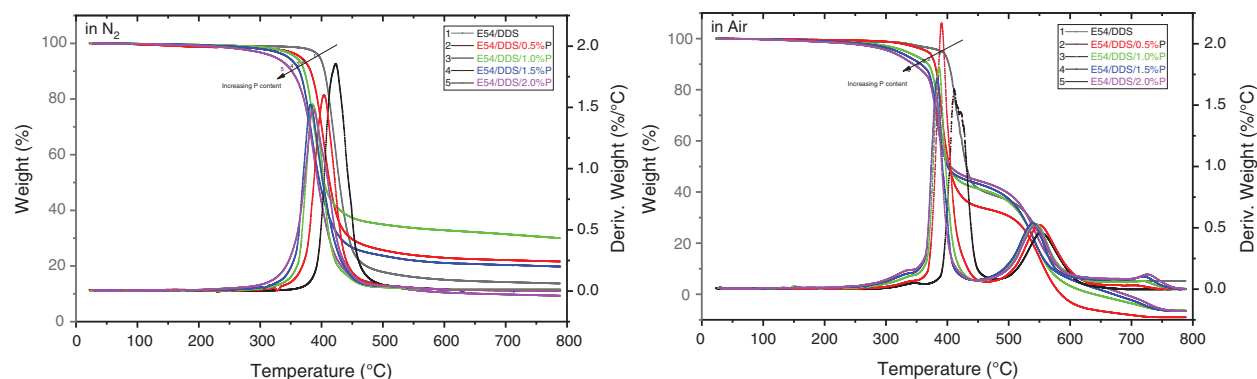


**Figure 3:** The thermogravimetric analytic curve of the epoxy thermosets in nitrogen and air at different flame-retardant loading (based on phosphorus content)

**Table 3:** Thermal stability of epoxy thermosets in N<sub>2</sub> and in the air and their LOI values

Entry	$T_{\text{onset}}/^{\circ}\text{C}$ N <sub>2</sub> (air)	$T_{\text{d5}}/^{\circ}\text{C}$ N <sub>2</sub> (air)	$T_{\text{dmax}}$ N <sub>2</sub> (air)	Residual/% 750°C/N <sub>2</sub> (air)	LOI/%	VL 94
E54/DDS	403 (399)	397 (390)	423 (411)	13.9 (5.1)	22.6	Fail
E54/DDS/0.5%P	383 (379)	366 (367)	404 (391)	21.8 (0)	30.3	V0
E54/DDS/1.0%P	376 (374)	358 (332)	386 (386)	30.6 (0)	32.5	V0
E54/DDS/1.5%P	364 (369)	346 (318)	382 (383)	20.0 (0)	28.5	V0
E54/DDS/2.0%P	363 (367)	324 (306)	389 (382)	9.5 (0)	29.3	V0

### 3.4 Flammability Analysis

The flame retardancy of the epoxy materials is characterized by limiting oxygen index (LOI) and from UL94 vertical burning tests. See Table 3 for the detailed results. When the epoxy contains only 0.5 wt% phosphorus (E54/DDS/1.0%P), its LOI increases from 22.6% for the unmodified (E54/DDS) to 30.3%. At the same time, the corresponding UL94 classification is greatly enhanced from no level to V0 grade. It can be concluded that DOPO-GE is an effective flame retardant for epoxy under the condition of relatively low loadings. When the phosphorus content in the system increased to 1.0 wt%, the flame retardancy of the materials is further improved, and the LOI is as high as 32.5%. However, as the loading of DOPO-GE continues to increase, the LOI decreases. This finding suggests that the phosphorus content has an optimal value, about 1.0%. Because too high DOPO-GE loading may weaken the carbonization ability of the thermosets and reduce the strength of the carbon structure formed during combustion.

By using a cone calorimeter to monitor combustion of the epoxy, the characteristic parameters of the thermosets containing the flame retardants with the 0.5%P content are studied in a more quantitative and comparable way. Fig. 4 shows how the HRR (heat release rate), THR (Total heat release), mass loss and TSP (Total smoke production) changes with the heating time, and Table 4 lists the main results from this test. In Fig. 4A and Table 4, pristine E54/DDS displays a slighter higher ignition time than E54/DDS/0.5%P does, due to the easy thermal decomposition of the flame retardant. However, the peak HRR value of E54/DDS/0.5%P is lower than that of E54/DDS ( $659 \pm 45$  vs.  $831 \pm 50$  kW m<sup>-2</sup>), with a 15.9% difference. The larger the HRR, the higher the fire intensity and the greater the danger of the material when catching fire. Thus, E54/DDS/0.5%P has the better flame retardancy than E54/DDS does.

In Fig. 4B, the THR of the thermoset increases over time, and eventually stabilizes indicating extinguishing. After 254 s, the THR value of the E54/DDS/0.5%P system is lower than that of E54/DDS, and finally reduces by 25.8%, implicating a reduction in the production of combustible volatiles. In Fig. 4C, E54/DDS/0.5%P shows a lower mass loss than DGEBA/DDS (65.99% vs. 86.75%) does, decreased by 24.0%. Because DOPO moieties in epoxy thermoset could catalyze the charring with the reduced gaseous combustible formation. The smoke generation is compared in Fig. 4D and Table 4. E54/DDS/0.5%P shows a decreased total smoke production (TSP) than E54/DDS does after ~290 s. As the ignition time increases, TSP increases rapidly, and finally the increase becomes sluggish and TSP tends to level off. Moreover, E54/DDS/0.5%P shows the much lower total smoke release (TSR) and total smoke production (TSP) values than E54/DDS does with a 22.2% reduction, indicating the decreased risk of fire hazard by suppressing smoke generation. The mechanisms of the enhanced flame retardancy and smoke depression are associated with increased charring ability and formation of protective char layers during combustion to form a tortuous pathway which slows down the mass and heat transfer and the free radical inhibition being in action in a gaseous phase [68–72].

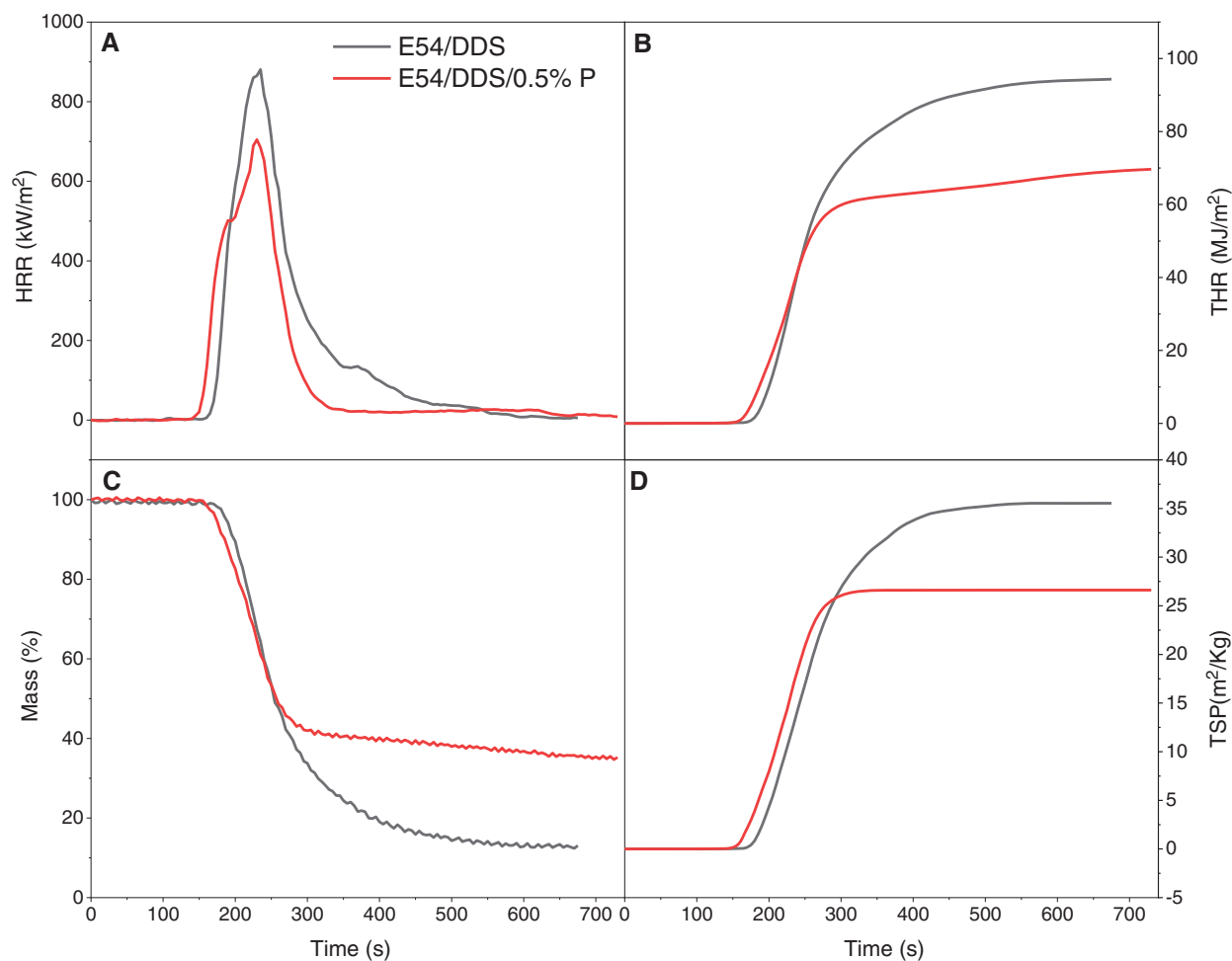


**Figure 4:** Cone calorimeter results of (A) heat release rate (HRR), (B) total heat release (THR), (C) specimen mass and (D) total smoke production (TSP) of the epoxy thermosets of E54/DDS and E54/DDS/0.5%P

**Table 4:** Main data obtained from cone calorimeter testing of E54/DDS and E54/DDS/0.5%P

	E54/DDS	E54/DDS/0.5%P
Time to ignition (s)	157.5 ± 0.5	132.5 ± 5.5
Peak HRR (kW m <sup>-2</sup> )	831 ± 50	659 ± 45
Total heat release (MJ m <sup>-2</sup> )	95.6 ± 1.45	67.8 ± 1.8
Mass loss (%)	86.75 ± 0.01	65.99 ± 0.01
Total smoke release (m <sup>2</sup> m <sup>-2</sup> )	4113 ± 95	3197 ± 190
Total smoke production (m <sup>2</sup> /Kg)	36.4 ± 0.83	28.3 ± 1.78

### 3.5 Morphology of Burnt Residual

Fig. 5 compares the effect of DOPO-GE on the epoxy thermosets with the different phosphorus content of 0, 1.0% and 1.5%, by highlighting the morphology of the residual obtained after combustion in air. Without addition of DOPO-GE, E54/DDS presents many large holes, due to the melting of the sample during the combustion process. In this case, once the sample is ignited, the generated heat will cause

rapid polymer chain scission leading to the melting and hole formation and produce a large amount of flammable gases. In this way, the diffusion of flammable gases and air and the heat transfer are greatly accelerated, which will promote the further decomposition and burning of the remaining epoxy matrix. After combustion in air, E54/DDS/1.0%P and E54/DDS/1.5%P show intumescent sponge-like morphology. The higher phosphorus content of the systems leads to the denser sponge morphology. This finding is likely due to the increased charring ability of the system to form porous carbon during the combustion process. The increased charring ability of the modified epoxy thermoset is due to the catalytic effect of phosphoric acid species formed during the pyrolysis. The formation of intumescent carbon structure will retard the diffusion of the flammables and heat transfer to underneath resin matrix, which will greatly slow down the combustion and even lead to self-extinguishing. These findings provide the further evidence for the better flame retardancy of the DOPO-GE-modified epoxy systems [8,73–75].

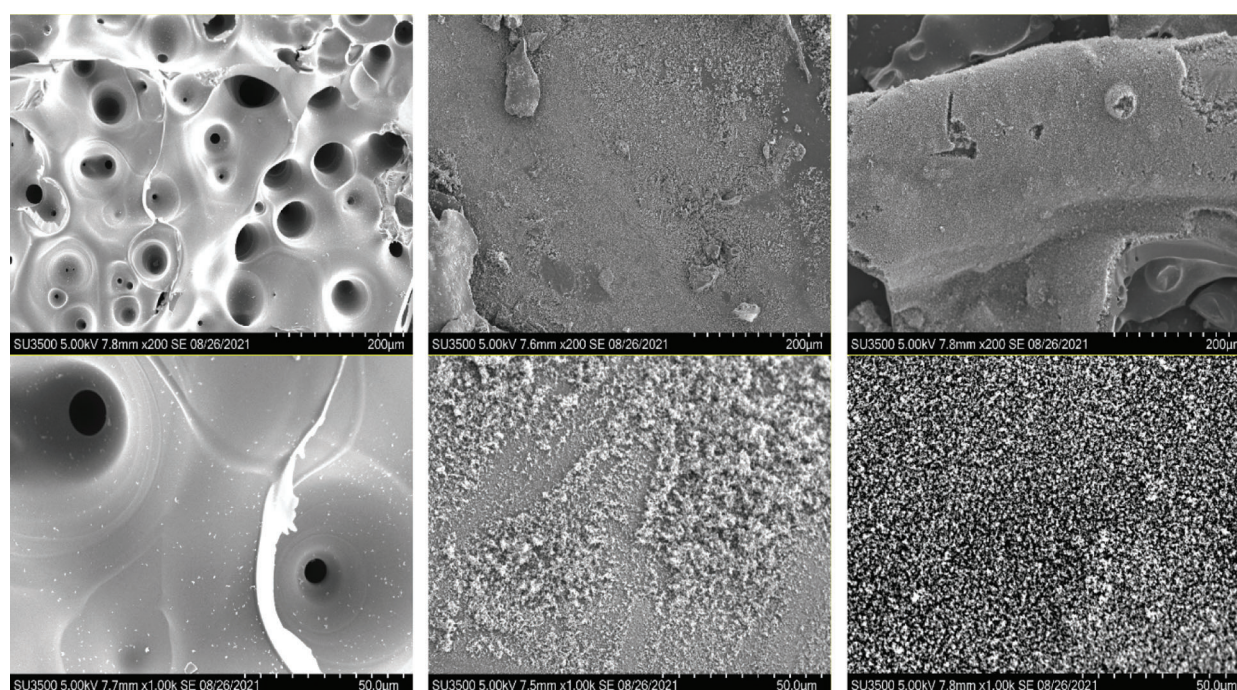


**Figure 5:** SEM images (200 times and 1000 times) of epoxy thermoset residual after combustion in air without (left) and with P contents of 1.0% (middle) and 1.5% (right)

### 3.6 Mechanical Performances of Thermosets

The mechanical properties of the thermosets are evaluated, and the effects of DOPO-GE on shear strength, impact strength, flexural modulus and fracture toughness and energy are investigated. The results in Table 5 show that with the increase of DOPO-GE loading, the flexural strength of the material increases. Especially, when the phosphorus content is 0.5 wt%, the flexural strength and modulus of the material increases from 183 to 281 MPa and from 2.34 to 3.98 GPa, respectively. Flexural properties of the material are improved, which is due to the improvement of the rigidity of the epoxy network. This is consistent with the results from the DMA results (Fig. 2). The impact strength decreases with an increase in the phosphorus content, which indicates that the plastic deformation of the material decreases under a high-speed impact stress. This may be related to the strong cohesive energy density of DOPO-GE in the epoxy system, which leads to an increase in the flexural properties, but makes the viscosity relaxation of the polymer chains more difficult. The decreased shear strengths are more likely related to the properties

of bonding surface such as wettability and surface energy. Also, the effects of DOPO-GE are investigated in terms of the fracture toughness ( $K_{IC}$ ) and fracture energy ( $G_{IC}$ ) of the thermosets.  $K_{IC}$  increases systematically from 2.4 to 4.9  $\text{MPa}\cdot\text{m}^{1/2}$ , as the phosphorus content increases from 0 to 2.0%. Meanwhile,  $G_{IC}$  arrives at the maximum of 5.7  $\text{MPa}\cdot\text{m}^{1/2}$  at 1.0% phosphorus content. This may be related to the increased the intermolecular interaction of the material to inhibit propagation of the cracks under a bending stress. Taken together, under the condition of the good flame-retardant performance, the phosphorus content of 0.5%–1.0% is a better choice to achieve well-balanced mechanical properties of the epoxy thermosets.

**Table 5:** Mechanical performances of E54/DDS thermoset with different DOPO-GE contents

Entry	Flexural strength/MPa	Flexural modulus/GPa	Shear strength/MPa	Impact strength/kJ/m <sup>2</sup>	$K_{IC}$ MPa·m <sup>1/2</sup>	$G_{IC}$ kJ/m <sup>2</sup>
E54/DDS	183 ± 2	2.34 ± 0.03	11.9 ± 0.1	2.52 ± 0.12	2.4 ± 0.1	4.2 ± 0.9
E54/DDS/0.5%P	234 ± 1	2.97 ± 0.09	10.9 ± 0.1	1.89 ± 0.28	3.2 ± 0.1	5.0 ± 0.4
E54/DDS/1.0%P	241 ± 2	3.69 ± 0.10	9.38 ± 0.09	1.56 ± 0.02	3.8 ± 0.1	5.7 ± 0.2
E54/DDS/1.5%P	251 ± 3	3.74 ± 0.13	8.53 ± 0.06	1.38 ± 0.19	4.7 ± 0.1	5.2 ± 0.1
E54/DDS/2.0%P	281 ± 2	3.98 ± 0.13	7.73 ± 0.09	1.06 ± 0.02	4.9 ± 0.2	4.9 ± 0.2

#### 4 Conclusions

By reacting glycidyl ether of eugenol with DOPO, a new bio-based halogen-free phosphorus flame retardant (DOPO-GE) was readily synthesized. Its molecular structure was characterized by FTIR and <sup>1</sup>H NMR. DOPO-GE was used to modify a bisphenol A epoxy prepolymer (E54) with DDS as the curing agent. DOPO-GE significantly reduced the glass transition temperature of the resultant thermosets, but increased the storage modulus. The cured epoxy material had high thermal stability. The onset thermal decomposition temperature in nitrogen and air exceeded 300°C. When the phosphorus content was 1.0 wt%, the residual content at 750°C in nitrogen increased from 13.9% for the unmodified epoxy to 30.6%. Therefore, the charring ability of the epoxy was greatly enhanced. When the phosphorus content was as low as 0.5 wt%, the LOI value could reach 30.3%, and the thermosets could pass the UL94 test with V0 level arrived. When the content of phosphorous content was increased to 1.0 wt%, LOI could further increase to 32.5%. Cone calorimeter results showed that the 0.5 wt% phosphorus incorporation in the epoxy led to the significantly decreased HRR (heat release rate), THR (total heat release) and TSP (Total smoke production), by 15.9%, 25.5% and 22.2%, respectively. The results of mechanical properties showed that the addition of DOPO-GE could significantly improve the flexural strength, modulus, fracture toughness, but could decrease the impact and shear strengths. In short, DOPO-GE is an effective halogen-free flame retardant derivable from renewable eugenol. When its loading is low (0.5–1.0 wt%, phosphorus based), DOPO-GE can effectively improve flame retardancy of the epoxy thermosets, and can enhance the rigidity of the epoxy network at the same time.

**Funding Statement:** The authors acknowledge the support from the National Natural Science Foundation of China (21875131 and 21773150), the Natural Science Basic Research Plan in Shaanxi Province of China (2020JM-283) and the Fundamental Research Funds for the Central Universities (GK202003044 and GK201902014).

**Conflicts of Interest:** The authors declare that they have no conflicts of interest to report regarding the present study.

## References

1. Huo, S., Song, P., Yu, B., Ran, S., Chevali, V. S. et al. (2021). Phosphorus-containing flame retardant epoxy thermosets: Recent advances and future perspectives. *Progress in Polymer Science*, 114, 101366. DOI 10.1016/j.progpolymsci.2021.101366.
2. Wang, X., Kalali, E. N., Wan, J. T., Wang, D. Y. (2017). Carbon-family materials for flame retardant polymeric materials. *Progress in Polymer Science*, 69, 22–46. DOI 10.1016/j.progpolymsci.2017.02.001.
3. Jin, F. L., Li, X., Park, S. J. (2015). Synthesis and application of epoxy resins: A review. *Journal of Industrial and Engineering Chemistry*, 29, 1–11. DOI 10.1016/j.jiec.2015.03.026.
4. Sai, T., Ran, S., Guo, Z., Yan, H., Zhang, Y. et al. (2021). Transparent, highly thermostable and flame retardant polycarbonate enabled by rod-like phosphorous-containing metal complex aggregates. *Chemical Engineering Journal*, 409(20), 128223. DOI 10.1016/j.cej.2020.128223.
5. Zhang, Y., Jing, J., Liu, T., Xi, L., Sai, T. et al. (2021). A molecularly engineered bioderived polyphosphate for enhanced flame retardant, UV-blocking and mechanical properties of poly(lactic acid). *Chemical Engineering Journal*, 411(7), 128493. DOI 10.1016/j.cej.2021.128493.
6. Yang, S., Huo, S., Wang, J., Zhang, B., Wang, J. et al. (2021). A highly fire-safe and smoke-suppressive single-component epoxy resin with switchable curing temperature and rapid curing rate. *Composites Part B: Engineering*, 207(4), 108601. DOI 10.1016/j.compositesb.2020.108601.
7. Peng, X., Li, Z., Wang, D., Li, Z., Liu, C. et al. (2021). A facile crosslinking strategy endows the traditional additive flame retardant with enormous flame retardancy improvement. *Chemical Engineering Journal*, 424, 130404. DOI 10.1016/j.cej.2021.130404.
8. Wang, X., Hu, Y., Song, L., Xing, W., Lu, H. et al. (2010). Flame retardancy and thermal degradation mechanism of epoxy resin composites based on a DOPO substituted organophosphorus oligomer. *Polymer*, 51(11), 2435–2445. DOI 10.1016/j.polymer.2010.03.053.
9. Mora, A. S., Tayouo, R., Boutevin, B., David, G., Caillol, S. (2019). Synthesis of biobased reactive hydroxyl amines by amination reaction of cardanol-based epoxy monomers. *European Polymer Journal*, 118(8), 429–436. DOI 10.1016/j.eurpolymj.2019.06.020.
10. Wazarkar, K., Sabnis, A. (2018). Cardanol based anhydride curing agent for epoxy coatings. *Progress in Organic Coatings*, 118, 9–21. DOI 10.1016/j.porgcoat.2018.01.018.
11. Wang, X., Zhou, S., Guo, W. W., Wang, P. L., Xing, W. et al. (2017). Renewable cardanol-based phosphate as a flame retardant toughening agent for epoxy resins. *ACS Sustainable Chemistry & Engineering*, 5(4), 3409–3416. DOI 10.1021/acssuschemeng.7b00062.
12. Wang, X., Niu, H., Guo, W., Song, L., Hu, Y. (2021). Cardanol as a versatile platform for fabrication of bio-based flame-retardant epoxy thermosets as DGEBA substitutes. *Chemical Engineering Journal*, 421(5), 129738. DOI 10.1016/j.cej.2021.129738.
13. Guo, W., Wang, X., Huang, J., Mu, X., Cai, W. et al. (2021). Phosphorylated cardanol-formaldehyde oligomers as flame-retardant and toughening agents for epoxy thermosets. *Chemical Engineering Journal*, 423, 130192. DOI 10.1016/j.cej.2021.130192.
14. Liu, J., Dai, J., Wang, S., Peng, Y., Cao, L. et al. (2020). Facile synthesis of bio-based reactive flame retardant from vanillin and guaiacol for epoxy resin. *Composites Part B: Engineering*, 190(22), 107926. DOI 10.1016/j.compositesb.2020.107926.
15. Fang, Z., Nikafshar, S., Hegg, E. L., Nejad, M. (2020). Biobased divanillin as a precursor for formulating biobased epoxy resin. *ACS Sustainable Chemistry & Engineering*, 8(24), 9095–9103. DOI 10.1021/acssuschemeng.0c02351.
16. Niu, H., Nabipour, H., Wang, X., Song, L., Hu, Y. (2021). Phosphorus-free vanillin-derived intrinsically flame-retardant epoxy thermoset with extremely low heat release rate and smoke emission. *ACS Sustainable Chemistry & Engineering*, 9(15), 5268–5277. DOI 10.1021/acssuschemeng.0c08302.
17. Qi, Y., Weng, Z., Kou, Y., Li, J., Cao, Q. et al. (2021). Facile synthesis of bio-based tetra-functional epoxy resin and its potential application as high-performance composite resin matrix. *Composites Part B: Engineering*, 214, 108749. DOI 10.1016/j.compositesb.2021.108749.

18. Qi, Y., Weng, Z., Zhang, K., Wang, J., Zhang, S. et al. (2020). Magnolol-based bio-epoxy resin with acceptable glass transition temperature, processability and flame retardancy. *Chemical Engineering Journal*, 387, 124115. DOI 10.1016/j.cej.2020.124115.
19. Nabipour, H., Qiu, S., Wang, X., Song, L., Hu, Y. (2021). Phosphorus-free ellagic acid-derived epoxy thermosets with intrinsic antflammability and high glass transition temperature. *ACS Sustainable Chemistry & Engineering*, 9(32), 10799–10808. DOI 10.1021/acssuschemeng.1c02434.
20. Nabipour, H., Wang, X., Song, L., Hu, Y. (2021). A high performance fully bio-based epoxy thermoset from a syringaldehyde-derived epoxy monomer cured by furan-derived amine. *Green Chemistry*, 23(1), 501–510. DOI 10.1039/D0GC03451G.
21. Zheng, J., Zhang, X., Cao, J., Chen, R., Aziz, T. et al. (2021). Behavior of epoxy resin filled with nano-SiO<sub>2</sub> treated with a eugenol epoxy silane. *Journal of Applied Polymer Science*, 138(14), 50138. DOI 10.1002/app.50138.
22. Liu, Y., Dai, J. Y., Liu, X. Q., Luo, J., You, S. S. et al. (2017). Bio-based epoxy resins derived from eugenol with low dielectric constant. *Journal of Electronic Packaging*, 139(3), 1082. DOI 10.1115/1.4036818.
23. Le, D., Samart, C., Kongparakul, S., Nomura, K. (2019). Synthesis of new polyesters by acyclic diene metathesis polymerization of bio-based  $\alpha,\omega$ -dienes prepared from eugenol and castor oil (undecenoate). *RSC Advances*, 9(18), 10245–10252. DOI 10.1039/C9RA01065C.
24. Harvey, B. G. (2017). Renewable resins and thermoplastics from eugenol. US9751991B1, USA.
25. Dai, J., Liu, X., Ma, S., Teng, N., Shen, X. et al. (2017). Preparation of eugenol-based organosilicon benzoxazine resin prepolymer. CN107417870A7.
26. Mattar, N., de Anda, A. R., Vahabi, H., Renard, E., Langlois, V. (2020). Resorcinol-based epoxy resins hardened with limonene and eugenol derivatives: From the synthesis of renewable diamines to the mechanical properties of biobased thermosets. *ACS Sustainable Chemistry & Engineering*, 8(34), 13064–13075. DOI 10.1021/acssuschemeng.0c04780.
27. Fang, L., Zhou, J., Wang, J., Sun, J., Fang, Q. (2018). A bio-based allylphenol (eugenol)-functionalized fluorinated maleimide with low dielectric constant and low water uptake. *Macromolecular Chemistry and Physics*, 219(20), 1800252. DOI 10.1002/macp.201800252.
28. Rios de Anda, A., Sotta, P., Modjinou, T., Langlois, V., Versace, D. L. et al. (2020). Multiscale structural characterization of biobased diallyl-eugenol polymer networks. *Macromolecules*, 53(6), 2187–2197. DOI 10.1021/acs.macromol.9b02280.
29. Ning, Y., Li, D. S., Wang, M. C., Chen, Y. C., Jiang, L. (2021). Bio-based hydroxymethylated eugenol modified bismaleimide resin and its high-temperature composites. *Journal of Applied Polymer Science*, 138(1), 49631. DOI 10.1002/app.49631.
30. Cui, X., Gu, G., Li, C., Liu, N., Gong, Y. et al. (2020). Synthesis and properties of biomass eugenol-functionalized isotactic poly(1-butene)s. *Polymer*, 202(1), 122739. DOI 10.1016/j.polymer.2020.122739.
31. Huang, M., Bai, D., Chen, Q., Zhao, C., Ren, T. et al. (2020). Facile preparation of polycarbonates from bio-based eugenol and 2-methoxy-4-vinylphenol. *Polymer Chemistry*, 11(32), 5133–5139. DOI 10.1039/D0PY00291G.
32. Naddeo, M., Vigliotta, G., Pellecchia, C., Pappalardo, D. (2020). Synthesis of bio-based polymacrolactones with pendant eugenol moieties as novel antimicrobial thermoplastic materials. *Reactive and Functional Polymers*, 155, 104714. DOI 10.1016/j.reactfunctpolym.2020.104714.
33. Mahajan, M. S., Mahulikar, P. P., Gite, V. V. (2020). Eugenol based renewable polyols for development of 2K anticorrosive polyurethane coatings. *Progress in Organic Coatings*, 148(12), 105826. DOI 10.1016/j.porgcoat.2020.105826.
34. Mattar, N., Rios de Anda, A., Vahabi, H., Renard, E., Langlois, V. (2020). Resorcinol-based epoxy resins hardened with limonene and eugenol derivatives: From the synthesis of renewable diamines to the mechanical properties of bio-based thermosets. *ACS Sustainable Chemistry & Engineering*, 8(34), 13064–13075. DOI 10.1021/acssuschemeng.0c04780.
35. Liu, L., Ni, Y., Zhi, Y., Zhao, W., Pudukudy, M. et al. (2020). Sustainable and biodegradable copolymers from SO<sub>2</sub> and renewable eugenol: A novel urea fertilizer coating material with superior slow release performance. *Macromolecules*, 53(3), 936–945. DOI 10.1021/acs.macromol.9b02202.

36. Shibata, M., Tetramoto, N., Imada, A., Neda, M., Sugimoto, S. (2013). Bio-based thermosetting bismaleimide resins using eugenol, bieugenol and eugenol novolac. *Reactive and Functional Polymers*, 73(8), 1086–1095. DOI 10.1016/j.reactfunctpolym.2013.05.002.
37. Harvey, B. G., Sahagun, C. M., Guenther, A. J., Groshens, T. J., Cambrea, L. R. et al. (2014). A high-performance renewable thermosetting resin derived from eugenol. *ChemSusChem*, 7(7), 1964–1969. DOI 10.1002/cssc.201400019.
38. Fang, L., Zhou, J., Tao, Y., Wang, Y., Chen, X. et al. (2019). Low dielectric fluorinated polynorborene with good thermostability and transparency derived from a biobased allylphenol (eugenol). *ACS Sustainable Chemistry & Engineering*, 7(4), 4078–4086. DOI 10.1021/acssuschemeng.8b05527.
39. Decostanzi, M., Tavernier, R., Fontaine, G., Bourbigot, S., Negrell, C. et al. (2019). Eugenol-based thermally stable thermosets by Alder-ene reaction: From synthesis to thermal degradation. *European Polymer Journal*, 117, 337–346. DOI 10.1016/j.eurpolymj.2019.05.018.
40. Bilel, H., Hamdi, N., Zagrouba, F., Fischmeister, C., Bruneau, C. (2012). Eugenol as a renewable feedstock for the production of polyfunctional alkenes via olefin cross-metathesis. *RSC Advances*, 2(25), 9584–9589. DOI 10.1039/c2ra21638h.
41. Li, C., Chen, Y., Cai, X., Yang, G., Sun, X. S. (2020). Eugenol-derived molecular glass: A promising biobased material in the design of self-healing polymeric materials. *ACS Sustainable Chemistry & Engineering*, 8(9), 3553–3560. DOI 10.1021/acssuschemeng.0c00397.
42. Hu, Y., Tian, Y., Cheng, J., Zhang, J. (2020). Synthesis of eugenol-based polyols via thiol-ene click reaction and high-performance thermosetting polyurethane therefrom. *ACS Sustainable Chemistry & Engineering*, 8(10), 4158–4166. DOI 10.1021/acssuschemeng.9b06867.
43. Liu, J., He, Z., Wu, G., Zhang, X., Zhao, C. et al. (2020). Synthesis of a novel nonflammable eugenol-based phosphazene epoxy resin with unique burned intumescent char. *Chemical Engineering Journal*, 390, 124620, 1–11. DOI 10.1016/j.cej.2020.124620.
44. Ruiz, Q., Pourchet, S., Placet, V., Plasseraud, L., Boni, G. (2020). New eco-friendly synthesized thermosets from isoeugenol-based epoxy resins. *Polymers*, 12(1), 229, 1–15. DOI 10.3390/polym12010229.
45. Tian, Y., Wang, Q., Cheng, J., Zhang, J. (2020). A fully biomass based monomer from itaconic acid and eugenol to build degradable thermosets via thiol-ene click chemistry. *Green Chemistry*, 22(3), 921–932. DOI 10.1039/C9GC03931G.
46. Hoefling, A., Nguyen, D. T., Lee, Y. J., Song, S. W., Theato, P. (2017). A sulfur-eugenol allyl ether copolymer: A material synthesized via inverse vulcanization from renewable resources and its application in li-s batteries. *Materials Chemistry Frontiers*, 1(9), 1818–1822. DOI 10.1039/C7QM00083A.
47. Periyasamy, T., Asrafali, S. P., Muthusamy, S. (2015). New benzoxazines containing polyhedral oligomeric silsesquioxane from eugenol, guaiacol and vanillin. *New Journal of Chemistry*, 39(3), 1691–1702. DOI 10.1039/C4NJ02047B.
48. Nal, P., Mestry, S., Mapari, S., Mhaske, S. (2019). Eugenol/vanillin-derived novel triarylmethane-based crosslinking agent for epoxy coating. *Iranian Polymer Journal*, 28(8), 685–695. DOI 10.1007/s13726-019-00736-0.
49. Chen, C. H., Tung, S. H., Jeng, R. J., Abu-Omar, M. M., Lin, C. H. (2019). A facile strategy to achieve fully bio-based epoxy thermosets from eugenol. *Green Chemistry*, 21(16), 4475–4488. DOI 10.1039/C9GC01184F.
50. Molina-Gutiérrez, S., Manseri, A., Ladmiral, V., Bongiovanni, R., Caillol, S. et al. (2019). Eugenol: A promising building block for synthesis of radically polymerizable monomers. *Macromolecular Chemistry and Physics*, 220(14), 1900179. DOI 10.1002/macp.201900179.
51. Wan, J., Gan, B., Li, C., Molina-Aldareguia, J., Kalali, E. N. et al. (2016). A sustainable, eugenol-derived epoxy resin with high biobased content, modulus, hardness and low flammability: Synthesis, curing kinetics and structure-property relationship. *Chemical Engineering Journal*, 284, 1080–1093. DOI 10.1016/j.cej.2015.09.031.
52. Krishnan, S., Arumugam, H., Chavali, M., Muthukaruppan, A. (2019). High dielectric, low curing with high thermally stable renewable eugenol-based polybenzoxazine matrices and nanocomposites. *Journal of Applied Polymer Science*, 136(6), 47050. DOI 10.1002/app.47050.
53. Chen, B., Wang, F., Li, J. Y., Zhang, J. L., Zhang, Y. et al. (2019). Synthesis of eugenol bio-based reactive epoxy diluent and study on the curing kinetics and properties of the epoxy resin system. *Chinese Journal of Polymer Science*, 37(5), 500–508. DOI 10.1007/s10118-019-2210-7.

54. Zhang, Y., Li, Y., Wang, L., Gao, Z., Kessler, M. R. (2017). Synthesis and characterization of methacrylated eugenol as a sustainable reactive diluent for a maleinated acrylated epoxidized soybean oil resin. *ACS Sustainable Chemistry & Engineering*, 5(10), 8876–8883. DOI 10.1021/acssuschemeng.7b01673.
55. Chen, X., Fang, L., Chen, X., Zhou, J., Wang, J. et al. (2018). A low-dielectric polymer derived from a biorenewable phenol (eugenol). *ACS Sustainable Chemistry & Engineering*, 6(10), 13518–13523. DOI 10.1021/acssuschemeng.8b03594.
56. Miao, J. T., Yuan, L., Guan, Q., Liang, G., Gu, A. (2018). Biobased epoxy resin derived from eugenol with excellent integrated performance and high renewable carbon content. *Polymer International*, 67(9), 1194–1202. DOI 10.1002/pi.5621.
57. Cheng, C., Li, Y., Zhang, X., Li, J. (2017). Eugenol-based non-isocyanate polyurethane and polythiourethane. *Iranian Polymer Journal*, 26(11), 821–831. DOI 10.1007/s13726-017-0567-4.
58. Liu, T., Hao, C., Wang, L., Li, Y., Liu, W. et al. (2017). Eugenol-derived biobased epoxy: Shape memory, repairing, and recyclability. *Macromolecules*, 50(21), 8588–8597. DOI 10.1021/acs.macromol.7b01889.
59. Faye, I., Decostanzi, M., Ecochard, Y., Caillol, S. (2017). Eugenol bio-based epoxy thermosets: From cloves to applied materials. *Green Chemistry*, 19(21), 5236–5242. DOI 10.1039/C7GC02322G.
60. Miao, J. T., Yuan, L., Guan, Q. B., Liang, G. Z., Gu, A. J. (2017). Biobased heat resistant epoxy resin with extremely high biomass content from 2,5-furandicarboxylic acid and eugenol. *ACS Sustainable Chemistry & Engineering*, 5(8), 7003–7011. DOI 10.1021/acssuschemeng.7b01222.
61. Liu, K., Madbouly, S. A., Kessler, M. R. (2015). Biorenewable thermosetting copolymer based on soybean oil and eugenol. *European Polymer Journal*, 69(1), 16–28. DOI 10.1016/j.eurpolymj.2015.05.021.
62. Modjinou, T., Versace, D. L., Abbad-Andallousi, S., Bousserhine, N., Dubot, P. et al. (2016). Antibacterial and antioxidant bio-based networks derived from eugenol using photo-activated thiol-ene reaction. *Reactive and Functional Polymers*, 101, 47–53. DOI 10.1016/j.reactfunctpolym.2016.02.002.
63. Ecochard, Y., Decostanzi, M., Negrell, C., Sonnier, R., Caillol, S. (2019). Cardanol and eugenol based flame retardant epoxy monomers for thermostable networks. *Molecules*, 24(9), 1818. DOI 10.3390/molecules24091818.
64. Pourchet, S., Sonnier, R., Ben-Abdelkader, M., Gaillard, Y., Ruiz, Q. et al. (2019). New reactive isoeugenol based phosphate flame retardant: Toward green epoxy resins. *ACS Sustainable Chemistry & Engineering*, 7(16), 14074–14088. DOI 10.1021/acssuschemeng.9b02629.
65. Liu, T., Sun, L., Ou, R., Fan, Q., Li, L. et al. (2019). Flame retardant eugenol-based thiol-ene polymer networks with high mechanical strength and transparency. *Chemical Engineering Journal*, 368, 359–368. DOI 10.1016/j.cej.2019.02.200.
66. Li, C., Wan, J., Kalali, E. N., Fan, H., Wang, D. Y. (2015). Synthesis and characterization of functional eugenol derivative based layered double hydroxide and its use as a nanoflame-retardant in epoxy resin. *Journal of Materials Chemistry A*, 3(7), 3471–3479. DOI 10.1039/C4TA05740F.
67. Zhang, D., Jin, S., Wan, J., Wang, J., Li, Y. et al. (2021). A dieugenol-based epoxy monomer with high bio-based content, low viscosity and low flammability. *Materials Today Communications*, 29(17), 102846. DOI 10.1016/j.mtcomm.2021.102846.
68. Huo, S., Yang, S., Wang, J., Cheng, J., Zhang, Q. et al. (2020). A liquid phosphorus-containing imidazole derivative as flame-retardant curing agent for epoxy resin with enhanced thermal latency, mechanical, and flame-retardant performances. *Journal of Hazardous Materials*, 386, 121984. DOI 10.1016/j.jhazmat.2019.121984.
69. Fang, F., Huo, S., Shen, H., Ran, S., Wang, H. et al. (2020). A bio-based ionic complex with different oxidation states of phosphorus for reducing flammability and smoke release of epoxy resins. *Composites Communications*, 17(7), 104–108. DOI 10.1016/j.coco.2019.11.011.
70. Fang, F., Ran, S., Fang, Z., Song, P., Wang, H. (2019). Improved flame resistance and thermo-mechanical properties of epoxy resin nanocomposites from functionalized graphene oxide via self-assembly in water. *Composites Part B: Engineering*, 165, 406–416. DOI 10.1016/j.compositesb.2019.01.086.
71. Cheng, J., Wang, J., Yang, S., Zhang, Q., Huo, S. et al. (2019). Benzimidazolyl-substituted cyclotriphosphazene derivative as latent flame-retardant curing agent for one-component epoxy resin system with excellent comprehensive performance. *Composites Part B: Engineering*, 177(23), 107440. DOI 10.1016/j.compositesb.2019.107440.

72. Wan, J., Gan, B., Li, C., Molina-Aldareguia, J. M., Li, Z. et al. (2015). A novel biobased epoxy resin with high mechanical stiffness and low flammability: Synthesis, characterization and properties. *Journal of Materials Chemistry A*, 3(43), 21907–21921. DOI 10.1039/C5TA02939B.
73. Jing, J., Zhang, Y., Fang, Z. P., Wang, D. Y. (2018). Core-shell flame retardant/graphene oxide hybrid: A self-assembly strategy towards reducing fire hazard and improving toughness of polylactic acid. *Composites Science and Technology*, 165, 161–167. DOI 10.1016/j.compscitech.2018.06.024.
74. Xiong, Z., Zhang, Y., Du, X., Song, P., Fang, Z. (2019). Green and scalable fabrication of core-shell biobased flame retardants for reducing flammability of polylactic acid. *ACS Sustainable Chemistry & Engineering*, 7(9), 8954–8963. DOI 10.1021/acssuschemeng.9b01016.
75. Zhang, Y., Xiong, Z., Ge, H., Ni, L., Zhang, T. et al. (2020). Core-shell bioderived flame retardants based on chitosan/alginate coated ammonia polyphosphate for enhancing flame retardancy of polylactic acid. *ACS Sustainable Chemistry & Engineering*, 8(16), 6402–6412. DOI 10.1021/acssuschemeng.0c00634.